Saturation of resistivity and Kohler's rule in Ni-doped $La_{1.85}Sr_{0.15}CuO_4$ cuprate

A. Malinowski,[1] V. L. Bezusyy,[1,2] and P. Nowicki[1]
[1]*Institute of Physics, Polish Academy of Sciences, al. Lotników 32/46, 02-668 Warsaw, Poland*
[2]*International Laboratory of High Magnetic Fields and Low Temperatures, ul. Gajowicka 95, 53-421 Wroclaw, Poland*
(Received 12 May 2016; published 30 January 2017)

We present the results of electrical transport measurements of $La_{1.85}Sr_{0.15}Cu_{1-y}Ni_yO_4$ thin single-crystal films at magnetic fields up to 9 T. Adding Ni impurity with strong Coulomb scattering potential to a slightly underdoped cuprate makes the signs of resistivity saturation at $\rho_{\rm sat}$ visible in the measurement temperature window up to 350 K. Employing the parallel-resistor formalism reveals that $\rho_{\rm sat}$ is consistent with the classical Ioffe-Regel-Mott limit and changes with carrier concentration n as $\rho_{\rm sat} \propto 1/\sqrt{n}$. Thermopower measurements show that Ni tends to localize mobile carriers, decreasing their effective concentration as $n \cong 0.15 - y$. The classical unmodified Kohler's rule is fulfilled for magnetoresistance in the nonsuperconducting part of the phase diagram when applied to the ideal branch in the parallel-resistor model.

DOI: 10.1103/PhysRevB.95.014521

I. INTRODUCTION

Increasing evidence for well-defined quasiparticles in underdoped cuprates seems to corroborate a view that they are normal metals, only with a small Fermi surface. Fermi-Dirac statistics underlying the quantum oscillations [1], single-parameter – quadratic in energy ω and temperature T – scaling in optical conductivity $\sigma(\omega,T)$ [2], T^2 resistivity behavior extending over a substantial T region in clean systems [3], and fulfillment of Kohler's rule that is typical for normal metals in magnetotransport [4] are observations in favor of the Fermi-liquid scenario.

On the other hand, in cuprates with significant disorder manifested by large residual resistivity $\rho_{\rm res}$, pure T^2 resistivity dependence has not been reported so far, as for $Bi_2Sr_2CuO_{6+\delta}$ [3,5,6], or has been observed only at relatively narrow doping and T region, as in $La_{2-x}Sr_xCuO_4$ (LSCO) [3,7]. The clear violation of Kohler's scaling in underdoped LSCO and $YBa_2Cu_3O_7$ [8,9] (although not necessarily indicating a breakdown of the Fermi-liquid description [10]) has served almost as a hallmark of their peculiar normal-state properties for two decades.

In contrast to overdoped cuprates where a large cylindrical Fermi surface yields a carrier density $n = p + 1$ (with p the doping level) [11–13], the total volume of the Fermi surface in underdoped systems is a small fraction of the first Brillouin zone and corresponds to $n = p$ through Luttinger's theorem [14–17]. This small n should be reflected in zero-field transport. In normal metals, resistivity ρ saturates in the vicinity of the Ioffe-Regel-Mott limit $\rho_{\rm IRM}$, where the elastic mean free path $l_{\rm min}$ becomes comparable to interatomic distance [18,19]. In cuprates, however, signs of saturation are seen at $\rho_{\rm sat}$ much larger than $\rho_{\rm IRM}$ calculated from the semiclassical Boltzmann theory [20–23]. Moreover, ρ (1000 K) ($\sim\rho_{\rm sat}$) in LSCO changes as $1/x$, while for $n \propto x$ [24], the theory predicts $\rho_{\rm sat} \propto 1/\sqrt{x}$.

The above can be explained by a breakdown of the quasiparticle picture due to strong inelastic scattering at high T manifested by the disappearing of a Drude peak in $\sigma(\omega)$ [23,25–27]. In systems where impurity scattering dominates the carrier relaxation (quasiparticle decay) rate $1/\tau$, the Drude peak is centered at $\omega = 0$ regardless of how strong scattering becomes [2,23]. Electron-electron interactions make τ frequency dependent but for Fermi-liquid-like ω^2 dependence, $\sigma(\omega)$ still peaks at $\omega = 0$ [2]. Thus large impurity-induced $\rho_{\rm res}$ may facilitate an approach to the Ioffe-Regel-Mott limit in dc ($\omega = 0$) LSCO transport at lower T before the spectral weight is transferred to higher-energy excitations at larger T. Ni impurity is a good candidate because its strong Coulomb scattering potential in the CuO_2 planes allows one to achieve large ρ at moderately high T [28,29].

In this paper, we report transport and thermopower measurements on slightly underdoped $x = 0.15$ LSCO with added Ni impurity. The obtained $\rho_{\rm sat}$ corresponds to the classical value for small Fermi surface and changes as $1/\sqrt{n}$. The Fermi-liquid quasiparticle picture holds in the nonsuperconducting part of the phase diagram, as revealed by $\rho \propto T^2$ dependence and classical Kohler's rule for magnetoresistance, both hidden under the large resistivity of the system.

II. RESULTS AND DISCUSSION

A. Experimental details

The four-point transport measurements were carried out on the c-axis-aligned single-crystal films grown on an isostructural $LaSrAlO_4$ substrate by the laser ablation method from the polycrystalline targets [30,31]. The thermopower, which is not sensitive to the grain boundaries and porosity effects in cuprates [32], was measured on the samples cut from the targets.

B. Zero-field transport

Figure 1 shows the systematic change in $\rho(T)$ with Ni, from the superconducting $y = 0$ specimen with midpoint $T_C = 34.6$ K to the $y = 0.08$ one exhibiting insulating behavior at low T. In high T, a change of slope in a portion of the $\rho(T)$ curves that increases with T foreruns the approaching saturation. Variation of $d\rho/dT$, visible even in the $y = 0$ data, authenticates the slope decreasing that becomes more pronounced with increasing y, as can be seen in Fig. 2(a). Resistivity in this region is described extremely well by the parallel-resistor formula

$$\frac{1}{\rho(T)} = \frac{1}{\rho_{id}(T)} + \frac{1}{\rho_{\rm sat}} = \frac{1}{a_0 + a_1 T + a_2 T^2} + \frac{1}{\rho_{\rm sat}}. \quad (1)$$

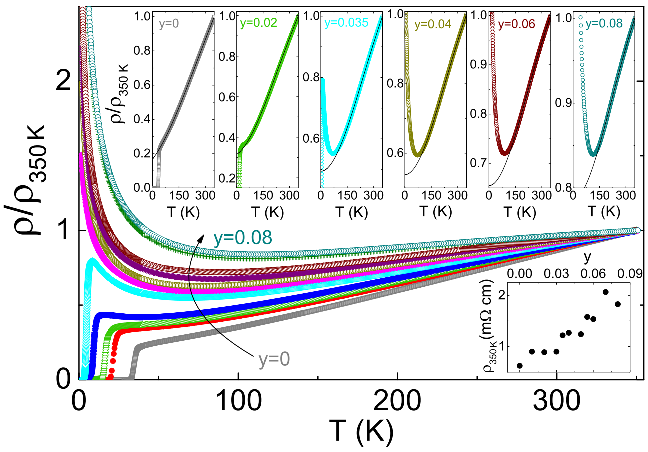

FIG. 1. Temperature dependence of normalized resistivity for a series of $La_{1.85}Sr_{0.15}Cu_{1-y}Ni_yO_4$ specimens. Their resistivities at $T = 350$ K are depicted in the lower inset. The upper inset shows the fits of Eq. (1) to 150–350 K data for selected specimens.

The ρ_{id} term is the ideal resistivity in the absence of saturation [19] and the additive-in-conductivity formalism stems from the existence of the minimal scattering time $\tau_{\min}$, equivalent to the Ioffe-Regel-Mott limit, which causes the shunt $\rho_{\rm sat}$ to always influence ρ in normal metals [33,34]. The formula was used for overdoped LSCO [35], but with the large-Fermi-surface $\rho_{\rm sat}$ value [34] as a fixed parameter. The excellent fits of Eq. (1) with all free parameters including $\rho_{\rm sat}$ to $\rho(T)$ in the 150–350 K interval are depicted in the upper inset to Fig. 1. Extending the fit interval downwards to lower T for small y does not significantly change the obtained fitting parameters, which are presented in Figs. 2(b)–2(d).

The Ni-induced residual resistivity, calculated as $1/\rho_{\rm res} = 1/\rho_{\rm sat} + 1/a_0$, accelerates with y such that at large y, it substantially exceeds the s-wave scattering unitarity limit $\Delta\rho_{\rm res} = (\hbar/e^2)(y/n)d$ for $n = 0.15 = $ const, depicted as a thin solid line in Fig. 2(b). Here, $d = c/2 \cong 6.6$ Å is the average separation of the CuO_2 planes in the $La_{1.85}Sr_{0.15}Cu_{1-y}Ni_yO_4$ films [31]. To find the actual $n(y)$ dependence, we carried out the thermopower measurements.

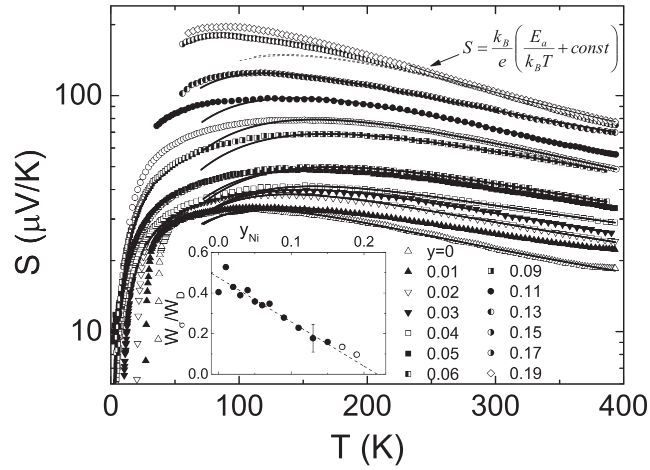

FIG. 3. Temperature dependence of Seebeck coefficient for $La_{1.85}Sr_{0.15}Cu_{1-y}Ni_yO_4$ from $y = 0$ (bottom) to $y = 0.19$ (top). The solid lines for $y \leqslant 0.15$ and the dashed ones for $y > 0.15$ are the best fits to the model from Ref. [40]. The thin solid line is the best fit of the thermally activated transport formula for $y = 0.19$. Inset: The W_σ/W_D ratio as a function of Ni doping. The dotted line is the best linear fit between $y = 0.02$ and 0.15.

Ni doping increases the positive Seebeck coefficient S, as can be seen in Fig. 3. Taking into account the universal correlation between S (290 K) and hole concentration fulfilled in most of the cuprate families [36–38], this strongly suggests a decreasing of carrier density with y. The $S(T)$ curves in $La_{1.85}Sr_{0.15}Cu_{1-y}Ni_yO_4$ retain the specific features of thermopower in underdoped cuprates: the initial strong growth of S with increasing T is followed by a broad maximum and subsequent slight decrease in S [39]. We find that the phenomenological asymmetrical narrow-band model [40] describes the experimental $S(T)$ curves very well at high T, above their maximum at $T_{\max}$. In this model, a sharp density-of-states peak with the effective bandwidth W_D is located near the Fermi level E_F and the carriers from the energy interval W_σ are responsible for conduction. In addition, a shift bW_D between the centers of W_D and W_σ bands is assumed. The best fits of the formula determining S in the model (Eq. (1) in Ref. [40]) are shown as thick lines in Fig. 3. The discrepancies at low T come from the limitations of the model derivated

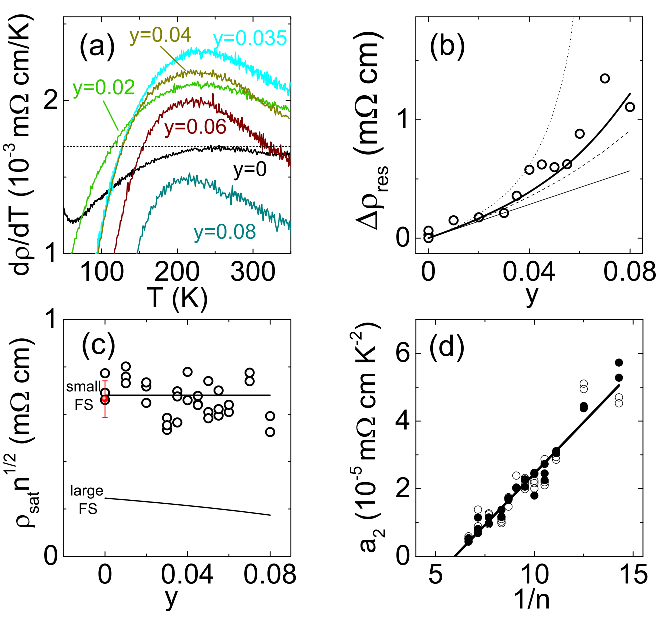

FIG. 2. (a) Temperature derivatives of $La_{1.85}Sr_{0.15}Cu_{1-y}Ni_yO_4$ resistivity. The dashed horizontal line is a guide to the eye. (b) The increase in residual resistivity of the samples with the smallest $\rho_{\rm res}$ for a given y. The lines show the unitarity limit assuming $n = 0.15 - y$ (thick line) and, for comparison, $n = 0.15$ (thin line), $n = 0.15 - 0.7y$ (dashed line), and hypothetical $n = 0.15 - 2y$ (dotted line). (c) The product $\rho_{\rm sat}\sqrt{n}$ with the arithmetic mean $(\rho_{\rm sat}\sqrt{n})_{av}$ (red dot) for the 32 measured samples. Solid lines show the expected y dependence for small and large Fermi surface. (d) The parameter a_2 as a function of inverse carrier concentration (open circles). Solid circles mark the normalized values $a_2^{\rm norm} = a_2(\rho_{\rm sat}\sqrt{n})_{av}/(\rho_{\rm sat}\sqrt{n})$ and the solid line is the linear fit to them.

under the assumption $W_D \cong k_B T$. Above $y = 0.15$, the model also fails for larger T, well above $T_{\max}$ ($W_D > 380$ meV, while $k_B T \cong 26$ meV at 300 K). For $y = 0.17$ and $y = 0.19$, S changes as $\propto 1/T$ above $\approx$250 K, consistent with the formula $S(T) = (k_B/e)(E_a/k_B T + \text{const})$ indicative of polarons. The thermal activation energy E_a estimated from the best fit for $y = 0.19$, $E_a = 32.4 \pm 0.2$ meV, is in good agreement with Ref. [41].

At the region of interest corresponding to high T, the asymmetrical narrow-band model works very well. The obtained asymmetry factor $b = -(0.06\text{–}0.08)$, although very small, is essential for good fits. The ratio F of n to the total number of states n_{DOS} is slightly above half filling (0.51–0.53) and thus consistent with the sign of S and in good agrement with literature data for $x = 0.15$ LSCO [40,42]. The Fermi level, $E_F = (F - 0.5)W_D - bW_D$, crosses the conduction-band upper edge at $y \approx 0.15$. The band filling F does not show any obvious y dependence. This means that Ni does not change n in the system (provided n_{DOS} remains constant). The primary effect of Ni doping appears to be *localization* of existing mobile carriers, as revealed by a decreasing of the W_σ/W_D ratio with increasing y (inset to Fig. 3). The ratio extrapolates to zero at $y = 0.22 \pm 0.02$, resulting in the average "localization rate" $\Delta n/\Delta y = 0.7 \pm 0.1$ hole/Ni ion. Employing the simple two-band model with the T-linear term [43], where the half width of the resonance peak Γ corresponds to the range of delocalized states, results in a similar physical picture. We found that Γ starts to decrease with increasing y above 0.07 and approaches zero for $y = 0.17$ [31]. The results are consistent with measurements of local distortion around Ni ions suggesting trapping hole by *each* Ni^{2+} [44] to create a well-localized Zhang-Rice doublet state [45], albeit they indicate a slightly lower $\Delta n/\Delta y$.

Having established the effective mobile carrier concentration $n \cong 0.15 - y$, we can revert to Fig. 2(b). As indicated by the thick solid line, scattering in the samples with the smallest ρ_{res} is in the unitarity limit for nonmagnetic impurity. Even assuming $\Delta n/\Delta y = 0.7$ (and unitarity limit), at most only a 20% increase in ρ_{res} for $y = 0.08$ can be attributed to scattering on magnetic moments. Thus, while our previous finding of spin-glass behavior in the system [30] undoubtedly indicates that the magnetic role of Ni ions in the spin-1/2 network of the CuO_2 planes cannot be neglected, the scattering on Ni has a predominantly nonmagnetic origin [28].

In Fig. 2(c), we show that the fitted ρ_{sat} agrees unexpectedly with ρ_{IRM} calculated from Boltzmann theory for the small Fermi surface with n holes. Assuming a cylindrical surface with the height $2\pi/d$ and taking the Ioffe-Regel-Mott condition as $l_{\min} \approx a$ (i.e., $k_F l_{\min} \approx \pi$; see Refs. [46,47]), where a is the lattice parameter in the CuO_2 plane, one gets $\rho_{\text{IRM}}^{\text{small}} = (\sqrt{2\pi}\hbar/e^2)d/\sqrt{n} = 0.68/\sqrt{n}$ mΩcm [26]. This is clearly distinguishable from the large Fermi surface case, $\rho_{\text{IRM}}^{\text{large}} = 0.68/\sqrt{1+n}$, which is inapplicable to the system. A simple formal statistics for all 32 measured samples shows that the product $\rho_{\text{sat}}\sqrt{n}$ for $n = 0.15 - y$ has a distribution with mean $\cong$ median and zero skewness [48].

The precise location of the large-to-small Fermi-surface transition on the phase diagram of the cuprates is still under debate. In the bismuth-based family, the expected linear relationship between n estimated from T_C and from Luttinger count is obtained only assuming a large surface from overdoped specimens down to $p \cong 0.145$ inclusive [49]. In $La_{1.85}Sr_{0.15}Cu_{1-y}Ni_yO_4$, Ni doping effectively moves the system towards smaller p, but the smooth evolution of all the fitted $\rho(T)$ parameters down to $y = 0$ points toward a small Fermi surface at $p = 0.15$. This finding is consistent with recent Hall measurements in $YBa_2Cu_3O_y$ indicating that Fermi-surface reconstruction with decreasing doping ends sharply at $p = 0.16$ [16].

The T-linear coefficient in Eq. (1) for three $y = 0$ samples, $\alpha_1 = 0.93 - 1.0\,\mu\Omega$cm/K, is identical to that at $n_{cr} = 0.185 \pm 0.005$ where a change in LSCO transport coefficients was found when tracked from the overdoped side [35]. Evidently, α_1 is not sensitive to the disappearing of the antinodal regions during degradation/reconstruction of the large Fermi surface into arcs/pockets. The linear-in-T scattering is anisotropic in the CuO_2 plane [50] and its maximal level at $(\pi,0)$ for $\alpha_1 = 1\ \mu\Omega$cm/K is comparable [35] with the Planckian dissipation limit [51,52]. Decoherence of quasiparticle states beyond this limit seems to be a plausible explanation [35] of the negligible role of antinodal states in the conductivity. While α_1 vanishes for all specimens with $y \geq 0.035$, the T^2 coefficient a_2 changes linearly with $1/n$ (compare Ref. [3]) in the whole studied y range [Fig. 2(d)]. When extrapolated *outside* accessible n, a_2 approaches zero at $n_{cr} = 0.167 \pm 0.009$. With such estimated error, the result means that strictly linear $\rho(T)$ dependence (albeit masked by ρ_{sat}) in LSCO is observed from the underdoped side only at optimum doping. *Interpreting* this as an indication of the (antiferromagnetic) quantum critical point remains speculative since a_2 diverges at such a point [53–56].

C. Magnetoresistance and Kohler's rule

After using the parallel-resistor formalism in the zero-field transport description, we will employ it to the analysis of magnetoresistance in the sections below. In the strongly overdoped cuprates, magnetoresistance obeys Kohler's rule [9]. The relative change of resistivity in magnetic field B, $\Delta\rho/\rho_0$, is a unique function of B/ρ_0, where $\rho_0 \equiv \rho\,(B = 0\,\text{T})$. In a recent reanalysis of the $x = 0.09$ LSCO data from Ref. [9], the modified Kohler's rule was proposed [4]. The isotemperature *transverse* magnetoresistance vs B/ρ_0 curves appear to collapse onto a single curve when ρ_0 is replaced by $\rho_0 - \rho_{\text{res}}$. Here, we propose an alternative approach for considering the large LSCO resistivity in the magnetoresistance analysis.

At the lowest temperatures down to 2 K, all nonsuperconducting samples exhibit large and negative in-plane ($I \parallel ab$) magnetoresistance, both in the transverse (TMR, $B \perp ab$) and longitudinal (LMR, $B \parallel ab$) configuration [TMR ($B = 9\,$T) $\approx 5 \times 10^{-2}$ at 2 K] [31]. In the following, we focus on the high-T region where, for the whole y range studied, magnetoresistance in both configurations is positive and two orders of magnitude smaller than in the low-T region. The typical field dependence of resistivity at various temperatures is displayed for the $y = 0.06$ specimen in the right inset to Fig. 4(a). Above 35 K, ρ increases as B^2. Below 60 K, the positive TMR begins to decrease with decreasing T and

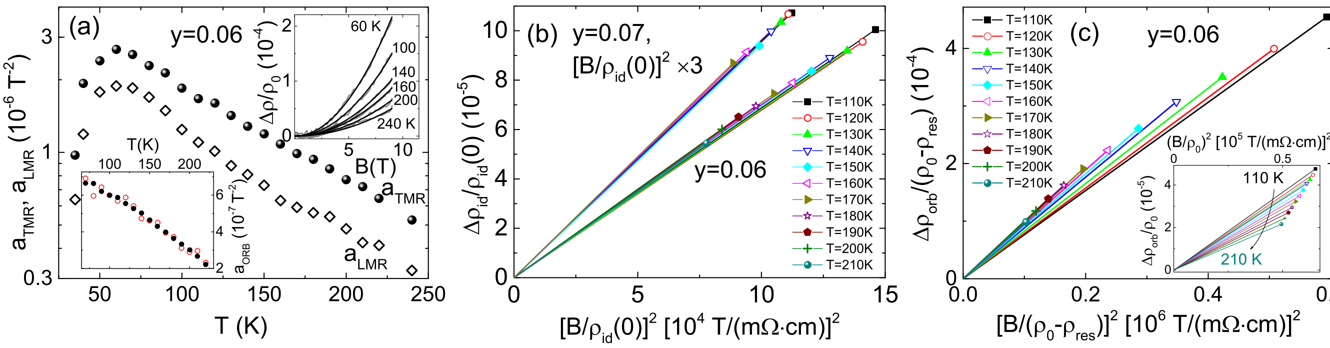

FIG. 4. Magnetoresistance of $y = 0.06$ specimen. (a) The temperature dependence of the coefficients a_{TMR} and a_{LMR}. The orbital part a_{ORB} (open symbols) and the result of its five-point adjacent averaging (solid symbols) are depicted in the left inset. The right inset shows B^2 fits to the TMR data at selected T. (b) Kohler scaling for the ideal branch, together with that of the $y = 0.07$ specimen for which the abscissa scale is enlarged three times. (c) Scaling approach from Ref. [4] and direct Kohler's-rule scaling attempt in inset.

smoothly evolves into a negative one at low T. Similar behavior is observed for LMR, which constitutes a significant portion of TMR (being equal to 60% of TMR at $T = 150$ K as an example) and thus may not be ignored in the analysis. To obtain the orbital part, OMR, at $T \geq 35$ K, we fitted $\rho(B)$ with the form $[\Delta\rho(B)/\rho(0)]_{TMR,LMR} = a_{TMR,LMR}B^2$ and next calculated $a_{ORB} = a_{TMR} - a_{LMR}$. The extracted coefficients are displayed in Fig. 4(a). A reliable and precise comparison of the various possible OMR scaling requires moderate numerical smoothing without alternating the a_{ORB} vs T dependence [left inset to Fig. 4(a)]. Employing the smoothed a_{ORB} coefficients, $a_{\rm orb}$, OMR at any field B can be calculated as OMR $= a_{\rm orb}B^2$.

Clearly, Kohler's rule in $La_{1.85}Sr_{0.15}Cu_{1-y}Ni_yO_4$ is violated when applied directly to the measured OMR of the specimen [inset to Fig. 4(c)]. Modification of the rule in the way described in Ref. [4] does not lead to any reasonable scaling range [57]. The $\Delta\rho_{\rm orb}/(\rho_0 - \rho_{\rm res})$ vs $[B/(\rho_0 - \rho_{\rm res})]^2$ lines collapse one onto another between 180 K and $T_{\rm up} = 200$ K, spanning only 10% of $T_{\rm up}$. Let us note that the existence of such a scaling—where the *whole* absolute resistivity change in field, $\Delta\rho_{\rm orb}$, is related only to the T-dependent $\rho_{el\text{-}ph} \equiv \rho_0 - \rho_{\rm res}$ part—would mean in the classical picture that the field acts between the scattering events only on these carriers that scatter against phonons during the subsequent scattering event and does not bend trajectories of those scattered against impurities.

The OMR analysis reveals that Kohler's rule in nonsuperconducting specimens is fulfilled in the ideal branch of the parallel-resistor model where the influence of the shunt $\rho_{\rm sat}$ is eliminated [Fig. 4(b)]. Interpreting the model in the spirit of the minimal τ_0 leads to the assumption that $\rho_{\rm sat}$ is field independent, at least in the weak-field regime (where actually observed OMR $\propto B^2$ dependence is expected). Fitting of Eq. (1) to $\rho(T)$ measured at various fields up to 9 T does not reveal any systematic change of $\rho_{\rm sat}$ with B [58]. With $\rho_{\rm sat}(B) = \rho_{\rm sat}(0)$, OMR of the ideal branch, $\Delta\rho_{id}/\rho_{id}(0)$, can be calculated from the measured quantities employing only one fitting parameter $\rho_{\rm sat}(0)$. The obtained $\Delta\rho_{id}/\rho_{id}(0)$ vs $[B/\rho_{id}(0)]^2$ curves from 110 K up to $T_{\rm up} = 210$ K collapse to a single temperature-independent line, spanning 50% of $T_{\rm up}$ [57]. A similar result was obtained for the $y = 0.07$ specimen. Closer to the superconducting region of the phase diagram, for $y = 0.04$, the scaling interval in $\rho_{id}(B,T)$ is much smaller (140–160 K), but a larger difference between $\rho_{\rm sat}$ and $\rho_{\rm res} \approx 0.3\rho_{\rm sat}$ emphasizes the difference between the possible OMR scalings, and the scaling approach illustrated in Fig. 4(c) fails completely.

III. CONCLUSIONS

The signs of resistivity saturation both at the value $\rho_{\rm IRM}$ and with n dependence from Boltzmann theory reflect the metalliclike character of transport despite a small volume of Fermi surface and strong disorder in underdoped LSCO. A fully quantum-mechanical explanation of saturation is still lacking [26,46,59–61]. Evidently, however, strong electron-electron interactions [62] do not invalidate the $\rho_{\rm IRM}$ limit [27]. The Ni-induced order-of-magnitude increase of the $a_0/\rho_{\rm sat}$ ratio leaves the resulting $\rho_{\rm IRM}^{\rm small}\sqrt{n}$ intact. The revealed omnipresence of $\tau_{\rm min}$ even in bad metals points towards the universality of the Ioffe-Regel-Mott criterion [46] rather than accidental-only agreement between $\rho_{\rm IRM}$ and saturation [27].

The known huge increase of ρ in LSCO outside our T-measurement window means the breakdown of quasiparticle description. At lower T, the transport in $La_{1.85}Sr_{0.15}Cu_{1-y}Ni_yO_4$ has a coherent description in the framework of Fermi-liquid theory, where Kohler's rule is derived under a single-relaxation-time approximation with the assumption of small τ anisotropy over the Fermi surface [63,64]. Fulfillment of the rule when ρ_0 is changed by changing temperature indicates nearly T-independent frequency distribution of the phonons involved [65] and is consistent with the Fermi-arc length in cuprates being constant [66,67] rather than decreasing with decreasing temperature [68]. Ni doping can restore antiferromagnetic fluctuations [30,69] that give additional T dependence in the magnetoresistance of nearly antiferromagnetic metals via correlation length $\xi_{AF}(T)$, OMR $\propto \xi_{AF}^4(T)\rho_0^{-2}$ [64]. Thus fulfillment of the conventional Kohler's rule suggests T-independent ξ_{AF} within the framework of this theory.

In summary, the parallel-resistor formalism that is typical for normal metals, employed for the analysis of

$La_{1.85}Sr_{0.15}Cu_{1-y}Ni_yO_4$ transport, reveals resistivity saturation at the value expected from Boltzmann theory for the small Fermi surface and fulfillment of the unmodified Kohler's rule in the nonsuperconducting part of the phase diagram.

ACKNOWLEDGMENT

This research was partially performed in the NanoFun laboratory cofinanced by the ERDF Project POIG.02.02.00-00-025/09.

[1] S. E. Sebastian, N. Harrison, M. M. Altarawneh, R. Liang, D. A. Bonn, W. N. Hardy, and G. G. Lonzarich, Phys. Rev. B **81**, 140505 (2010).

[2] S. I. Mirzaei, D. Stricker, J. N. Hancock, C. Berthod, A. Georges, E. van Heumen, M. K. Chan, X. Zhao, Y. Li, M. Greven *et al.*, Proc. Natl. Acad. Sci. USA **110**, 5774 (2013).

[3] N. Barišić, M. K. Chan, Y. Li, G. Yu, X. Zhao, M. Dressel, A. Smontara, and M. Greven, Proc. Natl. Acad. Sci. USA **110**, 12235 (2013).

[4] M. K. Chan, M. J. Veit, C. J. Dorow, Y. Ge, Y. Li, W. Tabis, Y. Tang, X. Zhao, N. Barišić, and M. Greven, Phys. Rev. Lett. **113**, 177005 (2014).

[5] H. Eisaki, N. Kaneko, D. L. Feng, A. Damascelli, P. K. Mang, K. M. Shen, Z.-X. Shen, and M. Greven, Phys. Rev. B **69**, 064512 (2004).

[6] Y. Ando, G. S. Boebinger, A. Passner, N. L. Wang, C. Geibel, and F. Steglich, Phys. Rev. Lett. **77**, 2065 (1996).

[7] Y. Ando, Y. Kurita, S. Komiya, S. Ono, and K. Segawa, Phys. Rev. Lett. **92**, 197001 (2004).

[8] J. M. Harris, Y. F. Yan, P. Matl, N. P. Ong, P. W. Anderson, T. Kimura, and K. Kitazawa, Phys. Rev. Lett. **75**, 1391 (1995).

[9] T. Kimura, S. Miyasaka, H. Takagi, K. Tamasaku, H. Eisaki, S. Uchida, K. Kitazawa, M. Hiroi, M. Sera, and N. Kobayashi, Phys. Rev. B **53**, 8733 (1996).

[10] R. H. McKenzie, J. S. Qualls, S. Y. Han, and J. S. Brooks, Phys. Rev. B **57**, 11854 (1998).

[11] M. Platé, J. D. F. Mottershead, I. S. Elfimov, D. C. Peets, R. Liang, D. A. Bonn, W. N. Hardy, S. Chiuzbaian, M. Falub, M. Shi *et al.*, Phys. Rev. Lett. **95**, 077001 (2005).

[12] B. Vignolle, A. Carrington, R. A. Cooper, M. M. J. French, A. P. Mackenzie, C. Jaudet, D. Vignolles, C. Proust, and N. E. Hussey, Nature (London) **455**, 952 (2008).

[13] B. Vignolle, D. Vignolles, D. LeBoeuf, S. Lepault, B. Ramshaw, R. Liang, D. Bonn, W. Hardy, N. Doiron-Leyraud, A. Carrington *et al.*, C. R. Phys. **12**, 446 (2011).

[14] N. Doiron-Leyraud, C. Proust, D. LeBoeuf, J. Levallois, J.-B. Bonnemaison, R. Liang, D. A. Bonn, W. N. Hardy, and L. Taillefer, Nature (London) **447**, 565 (2007).

[15] N. Barišić, S. Badoux, M. K. Chan, C. Dorow, W. Tabis, B. Vignolle, G. Yu, J. Beard, X. Zhao, C. Proust *et al.*, Nat. Phys. **9**, 761 (2013).

[16] S. Badoux, W. Tabis, F. Laliberté, G. Grissonnanche, B. Vignolle, D. Vignolles, J. Béard, D. A. Bonn, W. N. Hardy, R. Liang *et al.*, Nature (London) **531**, 210 (2016).

[17] S. Badoux, S. A. A. Afshar, B. Michon, A. Ouellet, S. Fortier, D. LeBoeuf, T. P. Croft, C. Lester, S. M. Hayden, H. Takagi *et al.*, Phys. Rev. X **6**, 021004 (2016).

[18] N. F. Mott, *Metal-Insulator Transition*, 2nd ed. (Taylor & Francis, London, 1990), Chap. 1, p. 30.

[19] H. Wiesmann, M. Gurvitch, H. Lutz, A. Ghosh, B. Schwarz, M. Strongin, P. B. Allen, and J. W. Halley, Phys. Rev. Lett. **38**, 782 (1977).

[20] J. Orenstein, G. A. Thomas, A. J. Millis, S. L. Cooper, D. H. Rapkine, T. Timusk, L. F. Schneemeyer, and J. V. Waszczak, Phys. Rev. B **42**, 6342 (1990).

[21] H. Takagi, B. Batlogg, H. L. Kao, J. Kwo, R. J. Cava, J. J. Krajewski, and W. F. Peck, Phys. Rev. Lett. **69**, 2975 (1992).

[22] N. L. Wang, B. Buschinger, C. Geibel, and F. Steglich, Phys. Rev. B **54**, 7445 (1996).

[23] K. Takenaka, J. Nohara, R. Shiozaki, and S. Sugai, Phys. Rev. B **68**, 134501 (2003).

[24] H. Takagi, T. Ido, S. Ishibashi, M. Uota, S. Uchida, and Y. Tokura, Phys. Rev. B **40**, 2254 (1989).

[25] K. Takenaka, R. Shiozaki, S. Okuyama, J. Nohara, A. Osuka, Y. Takayanagi, and S. Sugai, Phys. Rev. B **65**, 092405 (2002).

[26] O. Gunnarsson, M. Calandra, and J. E. Han, Rev. Mod. Phys. **75**, 1085 (2003).

[27] M. Calandra and O. Gunnarsson, Europhys. Lett. **61**, 88 (2003).

[28] E. W. Hudson, K. M. Lang, V. Madhavan, S. H. Pan, H. Eisaki, S. Uchida, and J. C. Davis, Nature (London) **411**, 920 (2001).

[29] Y. Tanabe, T. Adachi, K. Suzuki, Y. Koike, T. Kawamata, Risdiana, T. Suzuki, and I. Watanabe, Phys. Rev. B **83**, 144521 (2011).

[30] A. Malinowski, V. L. Bezusyy, R. Minikayev, P. Dziawa, Y. Syryanyy, and M. Sawicki, Phys. Rev. B **84**, 024409 (2011).

[31] A. Malinowski *et al.* (unpublished).

[32] A. Carrington and J. Cooper, Physica C: Superconductivity **219**, 119 (1994).

[33] M. Gurvitch, Phys. Rev. B **24**, 7404 (1981).

[34] N. E. Hussey, Eur. Phys. J. B **31**, 495 (2003).

[35] R. A. Cooper, Y. Wang, B. Vignolle, O. J. Lipscombe, S. M. Hayden, Y. Tanabe, T. Adachi, Y. Koike, M. Nohara, H. Takagi *et al.*, Science **323**, 603 (2009).

[36] S. D. Obertelli, J. R. Cooper, and J. L. Tallon, Phys. Rev. B **46**, 14928(R) (1992).

[37] T. Honma, P. H. Hor, H. H. Hsieh, and M. Tanimoto, Phys. Rev. B **70**, 214517 (2004).

[38] T. Kondo, T. Takeuchi, U. Mizutani, T. Yokoya, S. Tsuda, and S. Shin, Phys. Rev. B **72**, 024533 (2005).

[39] Due to technical problems with the thermopower measurements of high-resistance samples in a Quantum Design, Inc. PPMS system, some low-T results are not shown in Fig. 3. Only the results that are consistent regardless of the gain used are presented. See Fig. 1 in Application Note 1684-200, *Seebeck Artifact in Samples with Strongly Temperature Dependent Resistivity* by Quantum Design, Inc., where the raw low-T data for a $y = 0.11$ sample are displayed.

[40] M. V. Elizarova and V. E. Gasumyants, Phys. Rev. B **62**, 5989 (2000).

[41] M. Zhiqiang, X. Gaojie, Y. Hongjie, W. Bin, Q. Xueyin, and Z. Yuheng, Phys. Rev. B **58**, 15116 (1998).

[42] J.-S. Zhou and J. B. Goodenough, Phys. Rev. B **51**, 3104 (1995).

[43] L. Forró, J. Lukatela, and B. Keszei, Solid State Commun. **73**, 501 (1990).

[44] H. Hiraka, D. Matsumura, Y. Nishihata, J. Mizuki, and K. Yamada, Phys. Rev. Lett. **102**, 037002 (2009).

[45] F. C. Zhang and T. M. Rice, Phys. Rev. B **37**, 3759 (1988).

[46] N. E. Hussey, K. Takenaka, and H. Takagi, Philos. Mag. **84**, 2847 (2004).

[47] M. R. Graham, C. J. Adkins, H. Behar, and R. Rosenbaum, J. Phys.: Condens. Matter **10**, 809 (1998).

[48] The linear fit to $\rho_{\mathrm{sat}}\sqrt{n}(y)$ for $n = 0.15 - y$ has a small nonzero slope that vanishes for $n = 0.15 - 0.7y$, but the result should be taken with some caution because of relatively large scattering of data.

[49] Y. He, Y. Yin, M. Zech, A. Soumyanarayanan, M. M. Yee, T. Williams, M. C. Boyer, K. Chatterjee, W. D. Wise, I. Zeljkovic *et al.*, Science **344**, 608 (2014).

[50] M. Abdel-Jawad, M. P. Kennett, L. Balicas, A. Carrington, A. P. Mackenzie, R. H. McKenzie, and N. E. Hussey, Nat. Phys. **2**, 821 (2006).

[51] J. Zaanen, Nature (London) **430**, 512 (2004).

[52] C. C. Homes, S. V. Dordevic, M. Strongin, D. A. Bonn, R. Liang, W. N. Hardy, S. Komiya, Y. Ando, G. Yu, N. Kaneko *et al.*, Nature (London) **430**, 539 (2004).

[53] S. A. Grigera, R. S. Perry, A. J. Schofield, M. Chiao, S. R. Julian, G. G. Lonzarich, S. I. Ikeda, Y. Maeno, A. J. Millis, and A. P. Mackenzie, Science **294**, 329 (2001).

[54] P. Gegenwart, J. Custers, C. Geibel, K. Neumaier, T. Tayama, K. Tenya, O. Trovarelli, and F. Steglich, Phys. Rev. Lett. **89**, 056402 (2002).

[55] J. Paglione, M. A. Tanatar, D. G. Hawthorn, E. Boaknin, R. W. Hill, F. Ronning, M. Sutherland, L. Taillefer, C. Petrovic, and P. C. Canfield, Phys. Rev. Lett. **91**, 246405 (2003).

[56] A. Malinowski, M. F. Hundley, C. Capan, F. Ronning, R. Movshovich, N. O. Moreno, J. L. Sarrao, and J. D. Thompson, Phys. Rev. B **72**, 184506 (2005).

[57] The T range of the scaling has been found semiquantitatively as a maximal one for which adding a next measured T point outside this range does not broaden the existing angle between the outermost lines in the plot.

[58] The larger field is needed to unmask the possible B dependence of ρ_{sat} (when treated as a formal fitting parameter) that may be obscured inside small magnetoresistance of the system.

[59] M. Calandra and O. Gunnarsson, Phys. Rev. B **66**, 205105 (2002).

[60] P. B. Allen, Physica B: Condens. Matter **318**, 24 (2002).

[61] Y. Werman and E. Berg, Phys. Rev. B **93**, 075109 (2016).

[62] Even for large y, the electron-electron scattering aT^2 term at $T = 350$ K exceeds the T-independent Ni-induced a_0 term.

[63] J. M. Ziman, *Principles of the Theory of Solids*, 2nd ed. (Cambridge University Press, Cambridge, 1972), Chap. 7.

[64] H. Kontani, Rep. Prog. Phys. **71**, 026501 (2008).

[65] A. B. Pippard, *Magnetoresistance in Metals* (Cambridge University Press, Cambridge, 1989), p. 23.

[66] T. Kondo, A. D. Palczewski, Y. Hamaya, T. Takeuchi, J. S. Wen, Z. J. Xu, G. Gu, and A. Kaminski, Phys. Rev. Lett. **111**, 157003 (2013).

[67] A. Kaminski, T. Kondo, T. Takeuchi, and G. Gu, Philos. Mag. **95**, 453 (2015).

[68] A. Kanigel, M. R. Norman, M. Randeria, U. Chatterjee, S. Souma, A. Kaminski, H. M. Fretwell, S. Rosenkranz, M. Shi, T. Sato *et al.*, Nat. Phys. **2**, 447 (2006).

[69] K. Tsutsui, A. Toyama, T. Tohyama, and S. Maekawa, Phys. Rev. B **80**, 224519 (2009).